A Numerical Study on Prediction of Noise Characteristics Generated By a Propeller

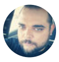

Ahmet Gultekin Avci
Istanbul Technical University

Emin Korkut
Istanbul Technical University

10th International Conference on Hydrodynamics
October 1-4, 2012 St. Petersburg, Russia

A Numerical Study on Prediction of Noise Characteristics Generated By a Propeller

Münir Cansın Özden[1], Ahmet Gültekin Avcı[1] and Emin Korkut[1*]
[1]Istanbul Technical University, Faculty of Naval Architecture and Ocean Engineering,
34469 Maslak-Istanbul, Turkey
[*]E-mail: korkutem@itu.edu.tr

ABSTRACT

Propulsion of surface and under water ships with low noise characteristics depends on a number of factors in terms of their safety and operational performances, and it is crucial to predict and control their underwater noise characteristics. In this respect, the main scope of this study is to calculate numerically the propeller noise, which is one of the main sources of underwater noise. Therefore, propeller noise is studied numerically and experimentally for non-cavitating conditions. Flow around the propeller is solved with a commercial CFD software, while hydro-acoustic analysis is performed using a model based on Ffowcs Williams-Hawking equation. In order to verify and validate numeric codes used in the analysis noise measurements were carried out for a navy vessel model propeller at Ata Nutku Cavitation Tunnel of Istanbul Technical University. This paper reports on preliminary results of the study. The paper includes the details of the study and tests conducted in the Ata Nutku Cavitation Tunnel and discusses further improvement of the methodology.

KEY WORDS: Propeller noise, prediction, Ffowcs Williams–Hawkings (FWH) model.

INTRODUCTION

Propeller is one of the most dominant sources of noise on ships. Propeller noise becomes the only traceable signal with sonars particularly for naval surface ships and submarines since all other sources can be eliminated by appropriate insulation methods. Nevertheless, it determines the detectability, operability and even survivability of the ship. Therefore, noise predictions for cavitating and non-cavitating propellers become a momentous subject of naval architecture for more than 50 years.

Empirical, semi-empirical methods and Bernoulli-based methods have been investigated by many researchers [1]. However, generation of a method by aero-acousticians Ffowcs Williams–Hawkings (FWH) for calculation of noise of an arbitrary body moving in a fluid can be considered a mile stone in acoustic predictions [2]. With the advancement of computing power and numerical practice, this method became available also for hydro-acoustic predictions. Seol et. al. [3] investigated the non-cavitating propeller noise employing Boundary Element Methods (BEM) for the calculation of flow around propeller in time-domain and used FWH method to predict the far-field acoustics. Seol et. al. [4] extended their work to cavitating noise stage. They predicted cavity extent by the sheet cavity volume model and used the sheet cavity volume data and time dependent pressure as the input for the FWH equation to predict far-field acoustics [4].

In 2003, Salvatore and Ianniello [5] published the preliminary results for cavitating propeller noise predictions. A hydrodynamic model for transient sheet cavitation on propellers in non–uniform inviscid flow was coupled with a hydroacoustic model based on the Ffowcs Williams–Hawkings equation. They split the noise signature into thickness and loading term contributions. They demonstrated that noise predictions by the FWH equation were in satisfactorily agreement with those obtained by using the Bernoulli equation model [5].

Barbarino and Casalino [6] studied and validated noise predictions for a NACA-0012 airfoil. Then they applied the same method to compute the broadband noise spectrum of an aircraft [6]. Gao et al. [7] simulated numerically the unsteady viscous flow around AUV with propellers by using the Reynolds-averaged Navier-Stokes (RANS) equations, shear-stress transport (SST) k-ω model and pressure with splitting of operators (PISO) algorithm based on sliding mesh. The hydrodynamic parameters of AUV with propellers such as resistance, pressure and velocity are got, which reflect well the real ambient flow field of AUV with propellers. Then, the semi-implicit method for pressure-linked equations (SIMPLE) algorithm is used to compute the steady viscous flow field of AUV hull and propellers, respectively. The computational results agree well with the experimental data, which shows that the numerical method has good accuracy in the prediction of hydrodynamic performance [7].

On the other hand, after the 22nd ITTC Workshop on Propeller RANS/Panel Methods, a number of studies have been published [8]. In 2004, Kawamura et. al. [9] comparatively analysed different turbulence models for the prediction of open water performance for a conventional propeller. Later Li published his results of estimating open water characteristics of a highly skewed model propeller employing k-ω turbulence model and validation study with experimental data [10]. The detailed literature review on the prediction of open water performance of propellers can be found in 26th ITTC [11].

In the above context a study has been carried out to investigate the prediction of propeller noise for surface ships and underwater vehicles. The main objective of the study is to obtain accurate propeller noise prediction and to use this information to control noise on ships. This paper presents the preliminary results of the study. A validation study for the open water performance and noise estimation of DTMB 4119 propeller has been carried out. The results obtained from the study are compared to those by Seol et. al. [3]. Studies continued with the calculation of acoustics for a highly skewed 5-bladed model navy vessel propeller and experiments performed at the Cavitation Tunnel of Ata Nutku Ship Model Testing Laboratory, Istanbul Technical University. Methodology used for the noise prediction is given in Methodology Section. Results of the study are included. Finally some conclusions withdrawn from the study are also given.

METHODOLOGY

Flow around a propeller is solved using a RANS solver with the SST k- ω turbulence model. Then, transient solution is performed with second order implicit pressure based solver. Velocity and pressure coupled via SIMPLE algorithm Numerical Methods and Flow Solver. Time dependent pressure data is used as the input for the FWH equation to predict far-field acoustics.

Numerical Methods and Flow Solver

For the numerical calculations ANSYS 13 Fluent is used to satisfy the following governing equation for continuity [12];

$$\frac{\partial \rho}{\partial t}+\frac{\partial}{\partial x_i}(\rho v_i)=0 \tag{1}$$

where x_i and $\boldsymbol{v_i}$ are the tensor form of axial coordinates and velocities, respectively. Then the momentum equation becomes;

$$\frac{\partial(\rho v_i)}{\partial t}+\frac{\partial(\rho u_i u_j)}{\partial x_j}= -\frac{\partial p}{\partial x_i}+\frac{\partial}{\partial x_j}\left[\mu\left(\frac{\partial u_i}{\partial x_j}+\frac{\partial u_j}{\partial x_i}-\frac{2}{3}\delta_{ij}\frac{\partial u_l}{\partial x_l}\right)\right] +\frac{\partial}{\partial x_j}\left(-\rho\overline{u_i' u_j'}\right) \tag{2}$$

where δ_{ij} is Kronecker Delta and $-\rho\overline{u_i' u_j'}$ are the unknown Reynolds stresses.

For the turbulence modelling, SST $k-\omega$ turbulence model is employed due to its good performance on wall bounded boundary layer flows [10].

FLUENT employs cell-centered finite volume method. RANS formulation is used with absolute velocity selection. Transient solution is performed with second order implicit pressure based solver. Velocity and pressure coupled via SIMPLE algorithm. Green Gauss Node Based is used for gradient and PRESTO for pressure discretizations. For Momentum, Turbulent Kinetic Energy and Specific Dissipation Rate calculations, QUICK scheme is selected.

Noise Predictions

Ffowcs Williams – Hawkings Method

Ffowcs Williams Hawkings (FWH) equation is an inhomogeneous wave equation derived from the continuity and Navier-Stokes equations [12].

$$\frac{1}{a_0^2}\frac{\partial^2 p'}{\partial t^2}-\nabla^2 p' = \frac{\partial^2}{\partial x_i \partial x_j}\{T_{ij}H(f)\}-\frac{\partial}{\partial t}\{[P_{ij}n_j + \rho u_i(u_n-v_n)]\delta(f)\}+\frac{\partial}{\partial t}\{[\rho_0 v_n+\rho(u_n-v_n)]\delta(f)\} \tag{3}$$

where

u_i: flow velocity in x_i direction
u_n: flow velocity normal to the surface ($f=0$)
v_i: surface velocity component in x_i direction
v_n: surface velocity component normal to the surface
$\delta(f)$: Dirac delta function
$H(f)$: Heaviside function

P’, is the far-field sound pressure ($p'=p-p_0$). $f=0$ is a mathematical surface used to facilitate the application of the generalised function theory and the free-space Green function to the unbounded space exterior flow problem ($f>0$) to reach the solution. This surface ($f=0$) represents a source (emission) surface and can be used as a suface overlapping with the body (impermeable) or as a permeable surface far from the body. n_i is the unit normal vector indicating the exterior region $(f = 0)$. a_0 is the sound velocity in the far field and T_{ij} is the Lighthill tensor defined as below [12];

$$T_{ij} = \rho u_i u_j + P_{ij} - a_0^2(\rho - \rho_0)\delta_{ij} \tag{4}$$

P_{ij} is the compressive stress tensor. For a Stokesian fluid it is defined as follows;

$$P_{ij} = p\delta_{ij} - \mu\left[\frac{\partial u_i}{\partial x_j} + \frac{\partial u_j}{\partial x_i} + \frac{2}{3}\frac{\partial u_k}{\partial x_k}\delta_{ij}\right] \tag{5}$$

The free-stream quantities are denoted by the subscript 0.

The solution of Eq. (4) is obtained by the use of the free-space Green function $(\delta(g)/4\pi r)$. The complete solution includes the surface and volume integrals. While the surface integrals include the effects of monopole, dipole and partially quadropole effects the volume integrals include only the quadropole sources except the regions of the source surface. In cases where the flow is in low subsonic region the value of the volume integral value diminishes and the source surface encloses the source region. Thus the volume integrals are not included to the calculations and the equations below are obtained [12];

$$p'(\vec{x},t) = p'_T(\vec{x},t) + p'_L(\vec{x},t) \tag{6}$$

where;

$$4\pi p'_T(\vec{x},t) = \int_{f=0}\left[\frac{\rho_0(\dot{U}_n + U_{\dot{n}})}{r(1-M_r)^2}\right]dS + \int_{f=0}\left[\frac{\rho_0 U_n\{r\dot{M}_r + a_0(M_r - M^2)\}}{r^2(1-M_r)^3}\right]dS \tag{7}$$

$$4\pi p'_L(\vec{x},t) = \frac{1}{a_0}\int_{f=0}\left[\frac{\dot{L}_r}{r(1-M_r)^2}\right]dS + \int_{f=0}\left[\frac{L_r - L_M}{r^2(1-M_r)^2}\right]dS + \frac{1}{a_0}\int_{f=0}\left[\frac{L_r\{r\dot{M}_r + a_0(M_r - M^2)\}}{r^2(1-M_r)^3}\right]dS \tag{8}$$

where;

$$U_i = v_i + \frac{\rho}{\rho_0}(u_i - v_i) \tag{9}$$

$$L_i = P_{ij}\hat{n}_j + \rho u_i(u_n - v_n) \tag{10}$$

When the integration surface is overlapping with a closed wall (impenetrable wall) the expressions $p'_T(\vec{x},t)$and $p'_L(\vec{x},t)$ from Eq. (7) and (8) are referred as the thickness noise term and the loading noise term [12]. The thickness noise term express the noise generated by the displacement of the flow and the loading noise term express the noise generated by the thrust generated by the rotation of the blade [1]. The terms in brackets in Eq. (7) and (8) express that the kernels of the integrals are solved for the retarded time steps (τ) expressed as in Eq. (11) where t is time and r is the observer distance;

$$\tau = t - \frac{r}{a_0} \tag{11}$$

The expressions in the equations denoted by a subscript are elements of vectors and unit vectors. For example $\hat{\vec{r}}$ and $\vec{n}$ denote the unit vectors in radiation and wall-normal directions in $L_r = \vec{L}\cdot\hat{\vec{r}} = L_i r_i$ and $U_n = \vec{U}\cdot\vec{n} = U_i n_i$. The dot over a variable denotes source-time differentiation of that variable [12].

Employing Ffowcs Williams Hawkings Method for the Prediction of Propeller Noise

FWHM becomes enabled when the solution is performed in ANSYS 13 Fluent, transiently. Propeller blade surfaces and hub is selected as the source of noise, and a number of receivers is defined for the measurements. For the calculations performed for DTMB4119, a total of 14 receivers located 10R away from the propeller reference point (0,0,0) and 0°, 45° and 90° angles from the shaft axis (x,0,0) and 30° angle steps from XY plane (Fig. 1). For the 5 bladed skewed propeller calculations, a total of 26 receivers were located 1m away from the propeller reference point with the same angles as the validation propeller. Acoustic data for 4 receiver locations are investigated within this paper. Locations for these receivers are given in Table 1.

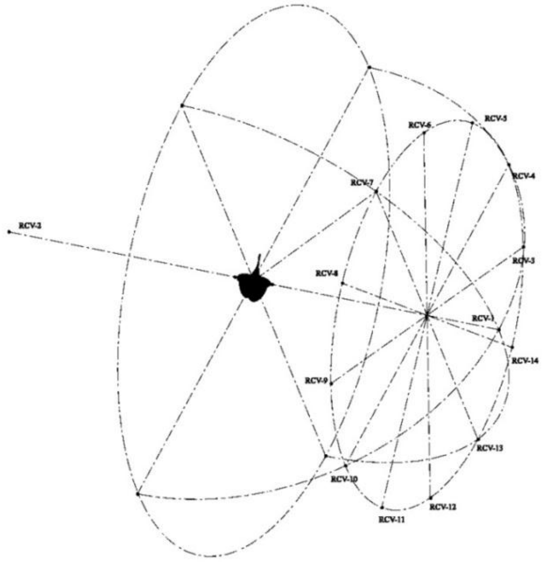

Fig. 1 Receiver locations for DTMB4119 propeller

Table 1. Receiver locations.

receiver-1	Shaft axis – 1 m forward
receiver-2	Shaft axis – 1m backward
receiver-3	Perpendicular to shaft axis - 1 m up
receiver-15	45° to shaft axis – upper side - 1m distance

Transient solution is initially performed for 0.001 time-steps for 5, 10 and 20 inner iterations. After noticing the negligible difference between different initial iterations 5 inner iterations is accepted to reduce the computational time.

Post processes of the solution are also performed by ANSYS 13 FLUENT by using Fast Fourier Transform properties. Hanning filter is used and results are shown for Sound Pressure Level (dB) form for 1/3 Octave band.

VALIDATION OF THE METHODOLOGY IN UNIFORM FLOW (PERFORMANCE AND NOISE PREDICTIONS)

In order to validate the methodology applied here DTMB4119 model propeller is used. Main particulars of the DTMB4119 propeller are given in Table 2.

Fig. 2 3D View of DTMB4119 Propeller used for validation process

Due to the transient form of the calculation, symmetry of the propeller blades was not used. Thus, the calculation domain was designed including all three blades of the propeller and hub. Tetrahedral elements are employed on the rotating inner domain and hexahedral elements for the stationary outer domain. Three different grid variations are generated and tested. Properties for the final grid selection for the calculations are listed in Table 3 and views of the domain and blade surfaces are given in Figs. 3 to 5.

Table 2. Main particulars of DTMB4119 propeller

Propeller Type / Model	DTMB 4119
Speed, U (m/s)	2.54
Propeller rate of rotation, N, (RPM)	600
Diameter, D (m)	0.3048 m
Direction of rotation	Right
Number of blades, Z	3
Expanded Blade Area Ratio, A_E/A_0	0.608
Hub-Diameter Ratio, r_h/R	0.2
Design Thrust Coefficient	0.150

Calculation is performed for the J values from 0.1 to 1.1. Steady solver is employed for the prediction of open water performances of the propeller. Results of K_T, K_Q and η_0 values are given in the Fig. 6 in comparison to the experimental values [13].

K_T values were predicted with a better accuracy than K_Q values. η_0 values were also affected by the prediction of K_Q values as expected. While the grid studies show that the finer the mesh, the accurate results can be predicted for the open water characteristics. However due to the much longer calculation times of transient solutions, finer grids did not used in this study.

Table 3. Final grid properties for validation propeller

Number of Nodes	4,004,777
Number of Elements	13,155,808

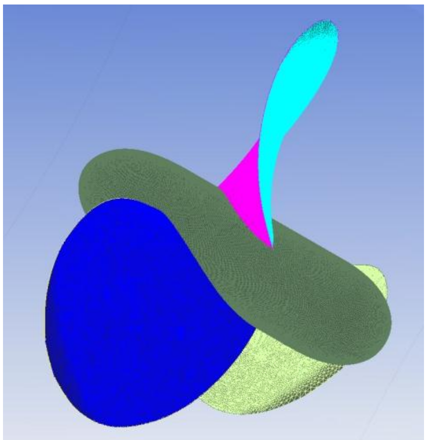

Fig. 3 Surface mesh on blades and hub

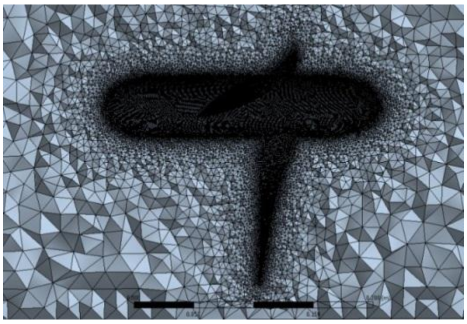

Fig. 4 Cutaway view of the mesh around propeller

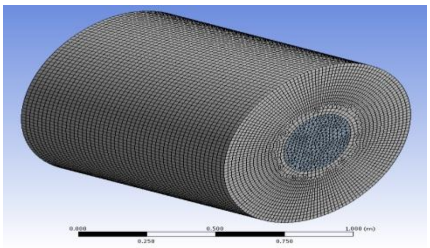

Fig. 5 General view of the calculation domain

After conducting steady state calculations, studies carried out for acoustic predictions which require time-domain pressure solutions. Solution for acoustic prediction of DTMB 4119 propeller operated at 120 RPM with a forward velocity of 1.6 m/s is given in Fig. 7 in comparison to those obtained by Seol et. al. [3]. Density and velocity of sound in the undisturbed medium for standard medium are 1026 kg/m^3 and 1500 m/s, respectively. The reference pressure for Sound Pressure Level calculations is 1 μPa.

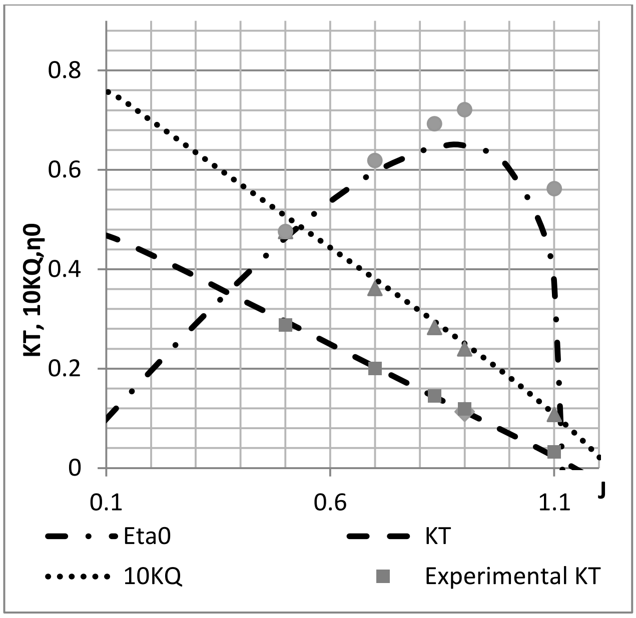

Fig. 6 Comparison of open water characteristics calculation for DTMB4119 with experimental results by [13]

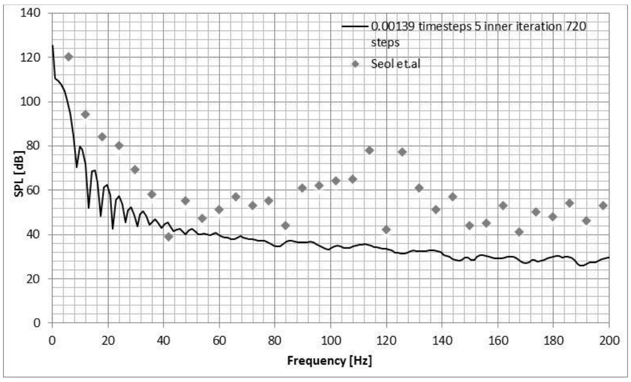

Fig. 7 Comparison of noise predictions for DTMB4119 propeller with those by Seol et al. [3].

PREDICTION OF NOISE CHARACTERISTICS FOR A SKEWED NAVY VESSEL PROPELLER

Main particulars and 3D views for the navy vessel propeller are given in Table 4 and Fig. 8, respectively.

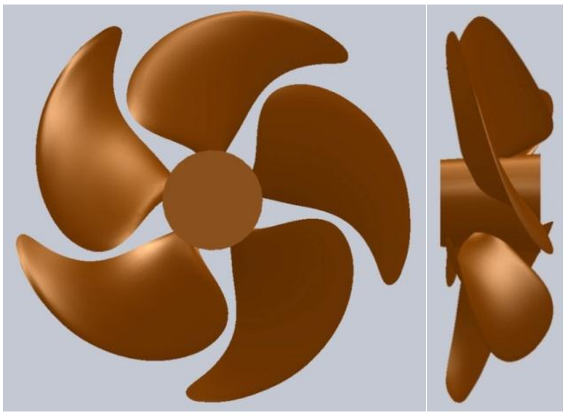

Fig. 8 3D views of the 5 bladed highly skewed navy vessel propeller

Table 4. Main particulars of navy vessel propeller

Speed, U (m/s)	3.16
Diameter, D, (m)	0.17
Pitch to Diameter ratio, P/D at 0.7R	1.222
A_E/A_0	0.850
Direction of rotation	Right
Number of blades, Z	5
J_{design}	0.925
Skew (degrees)	40
J values	0.905, 0.802, 0.598 and 0.504

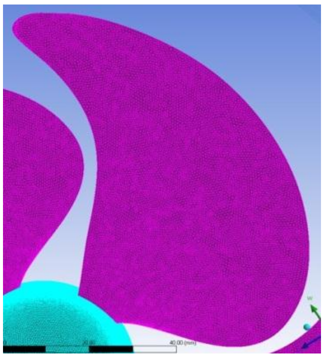

Fig. 9 Surface mesh for blades and hub

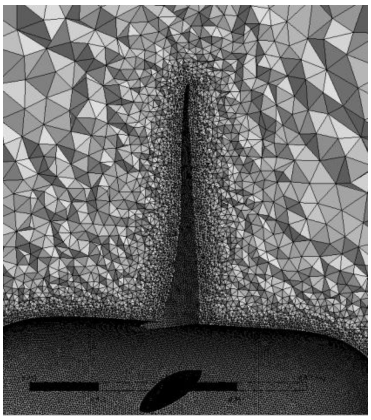

Fig. 10 Cutaway view of the mesh around propeller

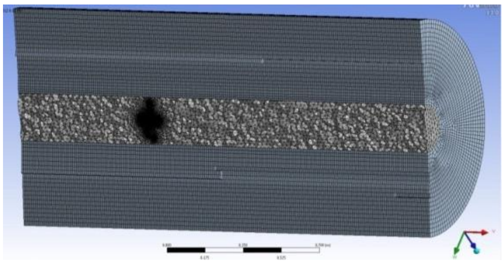

Fig. 11 General view of the calculation domain

After validation of the method by comparing its open water characteristics to the experimental results given by Brandner [13], and the noise predictions to those by Seol et.al. [3], studies carried out for a highly skewed 5 bladed navy vessel model propeller. Number of nodes and elements used in the analysis of noise prediction for the above propeller is given in Table 5.

Table 5. Grid properties employed for navy vessel propeller

Number of nodes	1,683,782
Number of elements	6,696,101

EXPERIMENTAL SETUP AND TEST CONDITIONS

Experiments have been conducted in the Cavitation Tunnel of Ata Nutku Ship Model Testing Laboratory, Istanbul Technical University. Dimensions of the larger section of the cavitation tunnel are 0.63mx0.35m (BxH).

It is normal practice in any cavitation tunnel to carry out background noise measurements with an idle mass in order to obtain the net propeller noise. Therefore the measurements were carried out first for the background noise, and then, for the propeller noise (propeller + background) at the following advance coefficients, J_1=0.905, J_2=0.802, J_3=0.598 and J_4=0.504. The measurements were recorded using a Bruel and Kjaer type 8103 miniature hydrophone mounted in a water filled, thick walled, steel cylinder placed on a Plexiglas window above the propeller at a vertical distance of 0.295m from the shaft centreline of the dynamometer that is shown in Fig. 12. The signals from the hydrophone were collected by further Bruel and Kjaer equipment, in this case a PC based 'Pulse' digital acquisition and analysis system up to a frequency of 25 kHz.

Tunnel water speed was set to 2 m/s and propeller rate of rotation were adjusted to obtain the advance coefficients given in Table 4 during the measurements. The model propeller used in the tests is shown in Fig. 13.

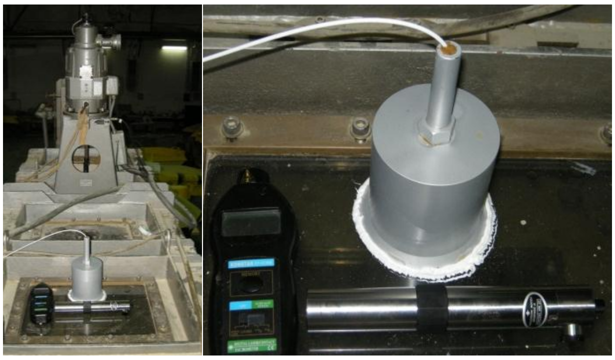

Fig. 12 Hydrophone arrangement on the cavitation tunnel

Fig. 13 Navy vessel model propeller with 5 blades and high skew

PRESENTATIONS AND DISCUSSIONS OF RESULTS

Computational fluid dynamics results for the prediction of acoustic properties for the 5 bladed highly skewed navy vessel propeller are given in Figs. 14 to 17 in comparison with the measured net noise of the model scale propeller.

A common practice in the analysis and presentation of the noise levels is to reduce the measured values of Sound Pressure Levels (SPL) in each 1/3 Octave band to an equivalent 1 Hz bandwidth by means of the correction formula recommended by ITTC (1978) as follows [14].

$$SPL_1 = SPL_m - 10log\Delta f \qquad (12)$$

where SPL_1 is the reduced sound pressure level to 1 Hz bandwidth in dB; re 1 μPa, SPL_m is the measured sound pressure level at each centre frequency in dB; re 1 μPa and Δf is the bandwidth for each one-third octave band filter in Hz. The ITTC also required that the sound pressure levels be corrected to a standard measuring distance of 1 m using the following relationship.

$$SPL = SPL_1 + 20log(r) \qquad (13)$$

where SPL is the equivalent 1 Hz at 1 m distance sound pressure level (dB; re 1 μPa) and r is the vertical reference distance for which the noise level was measured (r=0.295 m).

Primary measurements were performed to obtain the background noise of the general system, including noise generated by the impeller, dynamometer, flow, etc. For this evaluation an idle mass was attached to the shaft which had the same weight of the propeller.

Level of net sound pressure at each centre frequency, SPL_N, was calculated by subtracting corresponding background noise, SPL_B, from the total (i.e. propeller plus background) noise level, SPL_T, by using the following logarithmic subtraction formula given by Ross [15]:

$$SPL_N = 10log\left[10^{\left(\frac{SPL_T}{10}\right)} - 10^{\left(\frac{SPL_B}{10}\right)}\right] \tag{14}$$

The results of the analysed measurements are presented in Fig. 13 through 17. In each graph: the logarithmic-scaled x-axis represents the centre frequencies in Hz, while the linear-scaled y-axis represents the sound pressure levels in dB re 1 μPa (standard reference pressure for water), 1 Hz, 1m.

The Cavitation Tunnel is a steel structure, which is mounted on a special foundation. The facility can be specified as **"noisy"** in nature requiring careful measurement of the background noise contributed from the major sources, which are the surrounding environment, impeller and dynamometer. The frequencies of the structural vibration generated by the dynamometer and impeller were found to be effective in the low frequency region less than 100 Hz. Therefore, it is most likely that the noise levels due to the blade rate frequency ranging from 65 Hz to 117 Hz and its harmonics as well as those due to the structural vibration must be effective in this frequency region.

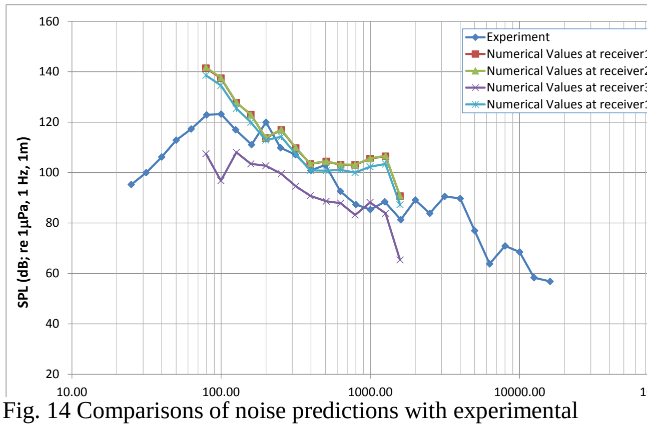

Fig. 14 Comparisons of noise predictions with experimental results at J=0.905

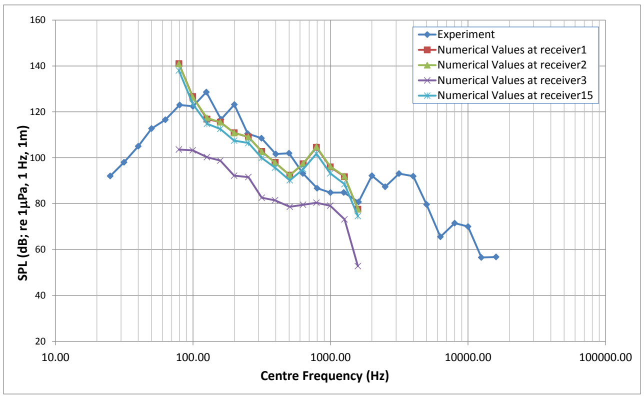

Fig. 15 Comparisons of noise predictions with experimental results at J=0.802

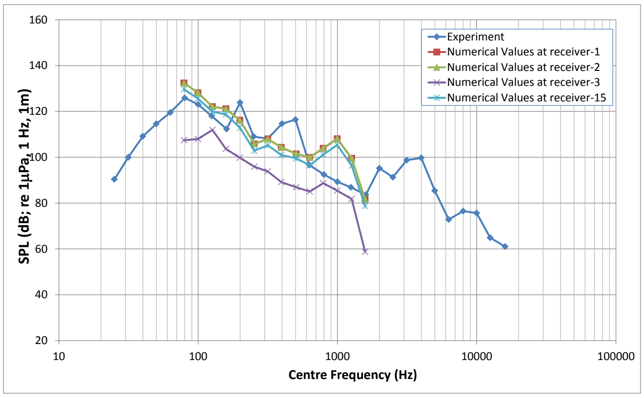

Fig. 16 Comparisons of noise predictions with experimental results at J=0.598

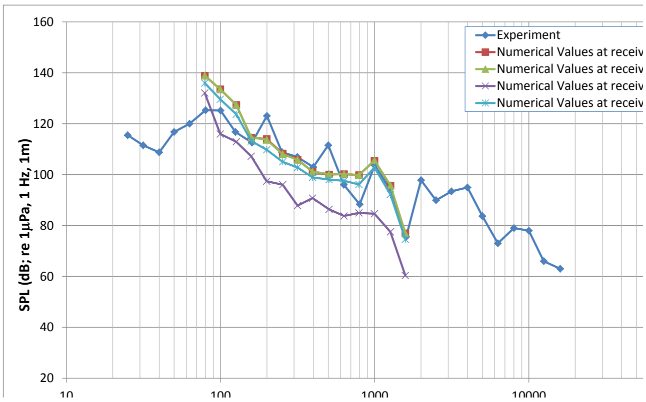

Fig. 17 Comparisons of noise predictions with experimental results at J=0.504

Comparisons of noise predictions for the receivers 1, 2 and 3 are in a good agreement with the experimental results. However for the receiver 15 there is a difference between the experiment and calculations, indicating that the calculation underpredicts the noise levels for the receiver with an angle to the shaft axis.

For the peak noise level in the low frequency range the numerical method applied over predicts slightly the propeller noise. This requires further tuning of the method to obtain more accurate noise levels.

During the noise measurements cavitation was not observed on the model propeller blades at the all advance coefficients.

CONCLUSIONS

A numerical and experimental study was carried out to predict propeller noise level for a navy vessel model propeller. Some conclusions drawn from the study are as follows:

- Open water performance of the validation propeller was well predicted, which was the input for the noise calculations.
- Noise levels of the propellers were satisfactorily predicted for majority of the receivers, except for the receiver with an angle to the shaft axis.
- The next step of the study is to include the cavitating stage of the noise prediction.
- In addition, effect of anti-fouling paint, namely environmentally friendly foul release systems, on the noise levels of propellers will be investigated numerically and experimentally as a future work.

ACKNOWLEDGEMENTS

This project was sponsored by the Technological and Research Council of Turkey (TUBITAK) with the project no: 110M327. The authors would like to thank to Assoc. Prof. A.C. Takinacı of ITU for providing data of DTMB4119. Prof. Ö. Gören, Assist. Prof. U.O. Ünal and Res. Assist. M. Özbulut of ITU are acknowledged for the help and use of the computational lab. The authors also thank to personnel of Ata Nutku Ship Model Testing Laboratory for their help during the experiments.

REFERENCES

[1] Testa, C. Acoustic formulations for aeronautical and rotorcraft noise prediction based on the Ffowcs Williams and Hawkings equation, Ph.D. Thesis, Universita degli Studi di ROMA TRE, Italy, Feb. 2008.
[2] Ffowcs Williams JE, Hawkings DL (1969) Sound generation by turbulence and surfaces in arbitrary motion. Philosophical Transactions of the Royal Society A264: 321–342.
[3] Seol, H., Suh, JC, Lee, S. Prediction of non-cavitating underwater propeller noise. J. Sound and Vibration. 2002, 257(1), 131-156.
[4] Seol, H., Suh, JC, Lee, S. Development of hybrid method for the prediction of underwater propeller noise. J. Sound and Vibration. 2005, 288(1), 345-360.
[5] Salvatore, F., Ianniello, S. Preliminary results on acoustic modelling of cavitating propellers. Comp. Mechanics. 2003, 32, 291–300
[6] Barbarino, M., Casalino, D. Hybrid analytical/numerical prediction of propeller broadband noise in time domain. Int. Jour. of Aeronautics. 2012, 11(2), 157–175.
[7] Gao, FD., Pan, CY, Han, YY. Numerical computation and analysis of unsteady viscous flow around autonomous underwater vehicle with propellers based on sliding mesh. J. of Central South University of Technology. 2012, 19(4), 944–952.
[8] ITTC. Propulsion Committee Report, Proceedings of the 25th ITTC, 25th International Towing Tank Conference. Fukuako, Japan, 2008, Vol. I, 83-141.
[9] Kawamura, T., Watanabe, T., Takekoshi, Y., Maeda, M., Yamaguchi, H. Numerical Simulation of Cavitating Flow around a Propeller, JSNA. 2004, Vol.195.
[10] Li, D.-Q. Validation of RANS predictions of open water performance of a highly skewed propeller with experiments. Conference of Global Chinese Scholars on Hydrodynamics, Journal of Hydrodynamics. 2006, 18(3), Supplement, 520-528.
[11] ITTC. Specialist Committee on Computational Fluid Dynamics Report, 26th International Towing Tank Conference. Rio de Janeiro, Brazil, 2011, 337-375.
[12] ANSYS 12 FLUENT Theory Guide. 2009.
[13] Brandner, P. Steady panel method analysis of DTMB 4119 propeller. Calculation results for the 22nd ITTC Propulsor Committee, Workshop on Propeller RANS/PANEL Methods. Houston, USA. 1999.
[14] ITTC. Cavitation Committee Report, 15th International Towing Tank Conference. The Hague, the Netherlands, 1978.
[15] Ross. Mechanics of underwater noise. Pergamon Press, New York, USA. 1976.